Suppl. Fig. 1. *Rap1* RNAi phenocopies the effects of Rap1 mutants. A-D. Embryos stained with antibodies to Rap1. A. Rap1 is already localized to the plasma membrane during syncytial stages. B,C. Rap1 localizes smoothly to the membrane all along the apical basal axis (B,C), thus overlapping but not co-localizing with spot AJs (B'). D. *Rap1* RNAi effectively reduces Rap1 levels below detection. E-G. Single apical-basal sections (E vs F) or projections (G vs H) reveal that *Rap1* RNAi reduces apical Arm enrichment (brackets) without causing loss in basal junctions (arrowheads). I-N. Single apical-basal sections (I vs F), apical views (J vs. M) or projections (L vs N) reveal that *Rap1* RNAi reduces apical Baz restriction (L vv N, brackets). O,P. *Rap1* RNAi leads to more variable apical cell area.

Suppl. Fig. 2. $Rap1^{MZ}$ mutants begin to lose epithelial integrity as development proceeds. A,B. Cuticle preparations of WT and $Rap1^{MZ}$ mutant. C-J. Late germband extension (stage 8) embryos. In wild-type, groups of cells in the epidermis round up and undergo synchronous divisions—cortical levels of AJ proteins (C) and Baz (F) are reduced in these cells. D. In cno^{MZ} mutants we previously found that once cells round up, they have difficulty regaining columnar cell shape, and thus rounded up cells with reduced apical AJ proteins accumulate (D,D close-up, brackets). E,F. In WT, while Baz is planar-polarized in the ectoderm, it still forms continuous junctions all around the cell, even in cells undergoing division (H, arrows). G,H. In presumptive zygotically rescued $Rap1^{M}$ mutants, while Baz continues to surround cells of the dorsal ectoderm, in the lateral ectoderm Baz at junctions becomes weak (red arrow) or fragmented (arrowheads). I,J. Even more severe defects are seen in presumptive $Rap1^{MZ}$ mutants, where Baz accumulation becomes highly fragmented in the lateral ectoderm (arrowheads). Scale bars=10μm.

Suppl. Fig. 3. Cno, Baz, AJ proteins, and aPKC localize to the membrane as early as syncytial divisions. WT embryos. A,H,L. Syncytial divisions (cycle 12/13). (A) Cno shows robust localization to pseudocleavage furrows during syncytial divisions. Arm (A') and Baz (H) also localize to psuedocleavage furrows at lower levels. aPKC (L) also displays membrane localization during syncytial divisions, when processed by formaldehyde fixation. B-G, J-K, M-O. Mid (B-D, J-K) or late (F,G) cellularization. Cno, DEcad/Arm, and Baz localize to spot AJs (C,D,K, arrows), DEcad/Arm also localize to basal junctions (O,

arrowhead), and Cno also accumulates apically early (D, arrowhead). aPKC remains membrane associated but localizes uniformly all along the lateral membrane (O). Scale bars=10μm.

Suppl. Fig 4. Rap1 and Cno play roles in Baz localization during gastrulation but other cues partially restore apical Baz in their absence. A-D. Plots displaying the average Baz image intensity in embryos of different genotypes (apical is to the left) at the indicated stages.

Suppl. Fig 5. Baz RNAi reduces Baz levels and mimics the effect of *baz* maternal and zygotic mutants. A-D. Maternal GAL4 driven *baz* RNAi effectively knocks down Baz, as assessed at gastrulation onset. In WT, Baz (A',C') is apically enriched and co-localizes with AJs (A, A'' brackets, C, C''). Unlike Baz, AJs are also basally enriched (A, A'' arrows, C inset). *baz* RNAi reduces Baz staining to background levels (B' vs. A'; D' vs. C') and disrupts apical accumulation of AJs (B'' bracket vs. A'' bracket). Scale bars=10μm.

Suppl. Fig. 6. In the absence of aPKC, Cno is not removed from the apical domain during gastrulation. A,B. Gastrulation onset (stage 6). C-H. Germband extension (stage 7). A-D. Loss of aPKC (B, D) leads to failure to exclude Cno apically (compare arrows), and reduced Cno coalescence along the apical-basal axis (compare brackets). During germband extension (stage 7) apical accumulation of Cno in *aPKC* mutants becomes more accentuated (E vs. F). G,H. In *aPKC* mutants, the belt AJs seen in WT (G) do not form—instead AJ proteins accumulate in puncta at the dorsal and ventral borders of cells (H' arrows). While the majority of Cno is located on the apical membrane in *aPKC* mutants (F), a portion co-localizes with these dorsal and ventral AJ puncta (H", arrows). Scale bars=10μm.

Suppl. Fig. 7. Rap1, Baz and aPKC play distinctive roles in maintaining columnar cell shape at gastrulation onset and during germband extension. Cell areas were measured at three different apical-basal depths during stage 6 or stage 7, as in Fig. 10, with mean CV values for each genotype and section. A-E. Representative stage 6 embryos, with mean CV values for each genotype and section. Arrows indicate examples of cell area variation. F-H. Bee-swarm scatter plots of cell areas. *Rap1, baz* RNAi, and *aPKC* all affect variability of apical cell area, while only *Rap1* significantly affects cell area variability in the most basal section. White lines=median value. I-M. Representative stage 7 embryos, with mean CV values. Arrows

indicate examples of variable cell areas. N-P. Bee-swarm scatter plots of cell areas. *Rap1, baz* RNAi, and *aPKC* all significantly affect variability of apical cell area. Scale bar=10μm.

Suppl. Fig. 8. Old and new models of polarity establishment. See text for details.

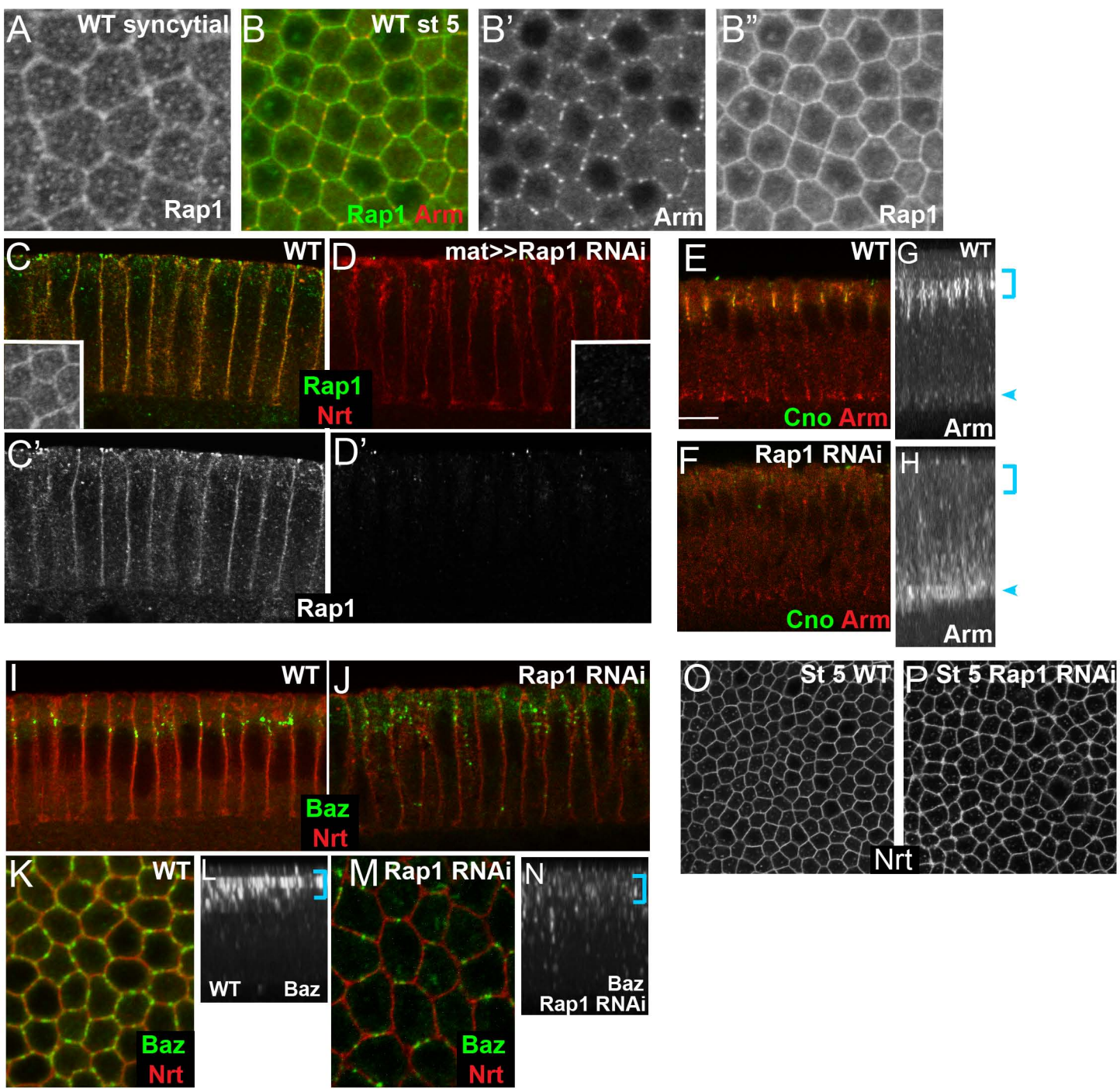
A
WT syncytial
Rap1
B
WT st 5
Rap1 Arm
B'
Arm
B"
Rap1
C
WT
D
mat>>Rap1 RNAi
Rap1
Nrt
C'
D'
Rap1
E
WT
Cno Arm
G
WT
Arm
F
Rap1 RNAi
Cno Arm
H
Arm
I
WT
J
Rap1 RNAi
Baz
Nrt
O
St 5 WT
P
St 5 Rap1 RNAi
Nrt
K
WT
Baz
Nrt
L
WT
Baz
M
Rap1 RNAi
Baz
Nrt
N
Baz
Rap1 RNAi

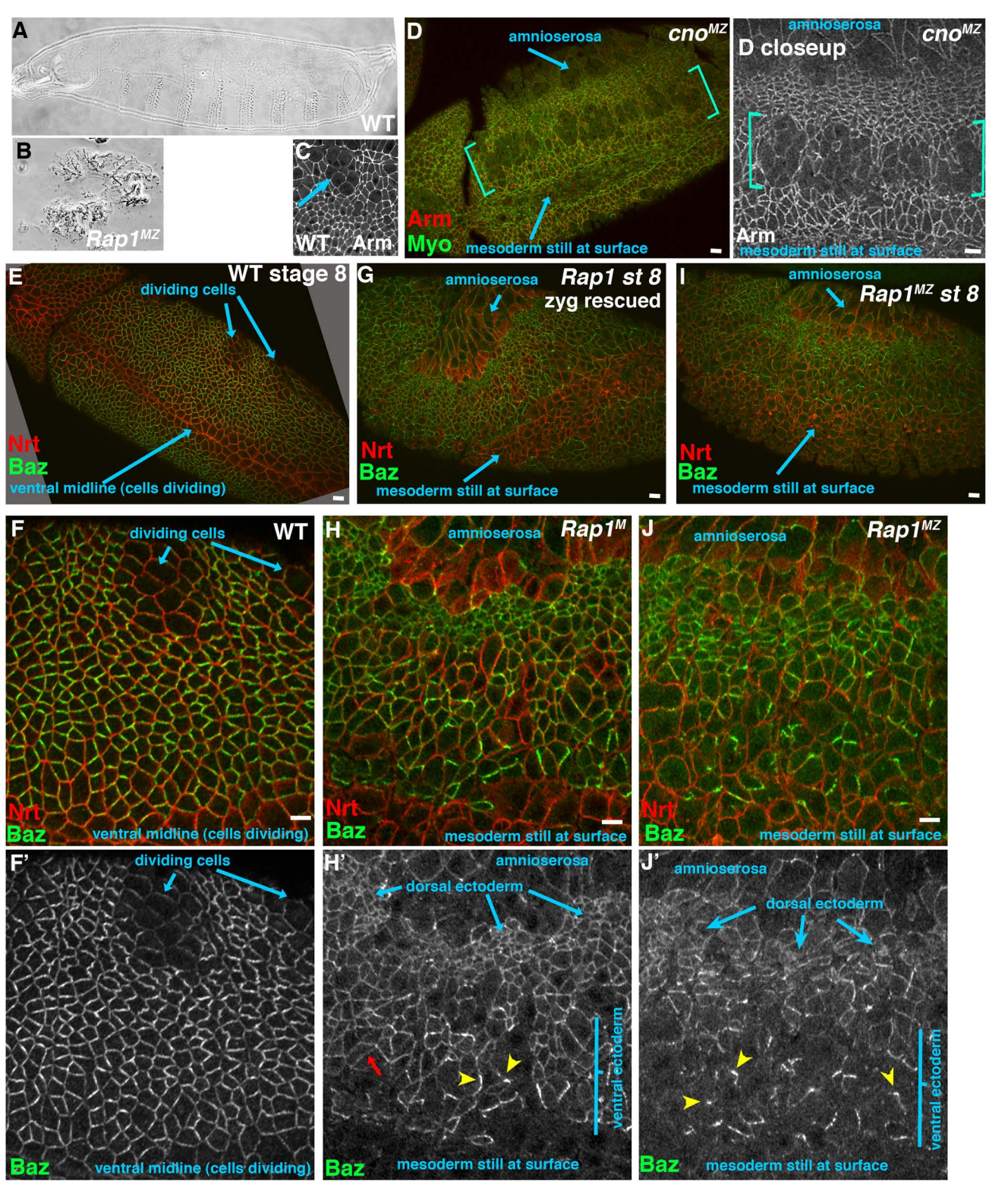
A
WT
B
Rap1MZ
C
WT Arm
D
amnioserosa
cnoMZ
Arm
Myo
mesoderm still at surface
D closeup
amnioserosa
cnoMZ
Arm
mesoderm still at surface
E
WT stage 8
dividing cells
Nrt
Baz
ventral midline (cells dividing)
G
amnioserosa
Rap1 st 8
zyg rescued
Nrt
Baz
mesoderm still at surface
I
amnioserosa
Rap1MZ st 8
Nrt
Baz
mesoderm still at surface
F
dividing cells
WT
Nrt
Baz
ventral midline (cells dividing)
H
amnioserosa
Rap1M
Nrt
Baz
mesoderm still at surface
J
amnioserosa
Rap1MZ
Nrt
Baz
mesoderm still at surface
F'
dividing cells
Baz
ventral midline (cells dividing)
H'
amnioserosa
dorsal ectoderm
ventral ectoderm
Baz
mesoderm still at surface
J'
amnioserosa
dorsal ectoderm
ventral ectoderm
Baz
mesoderm still at surface

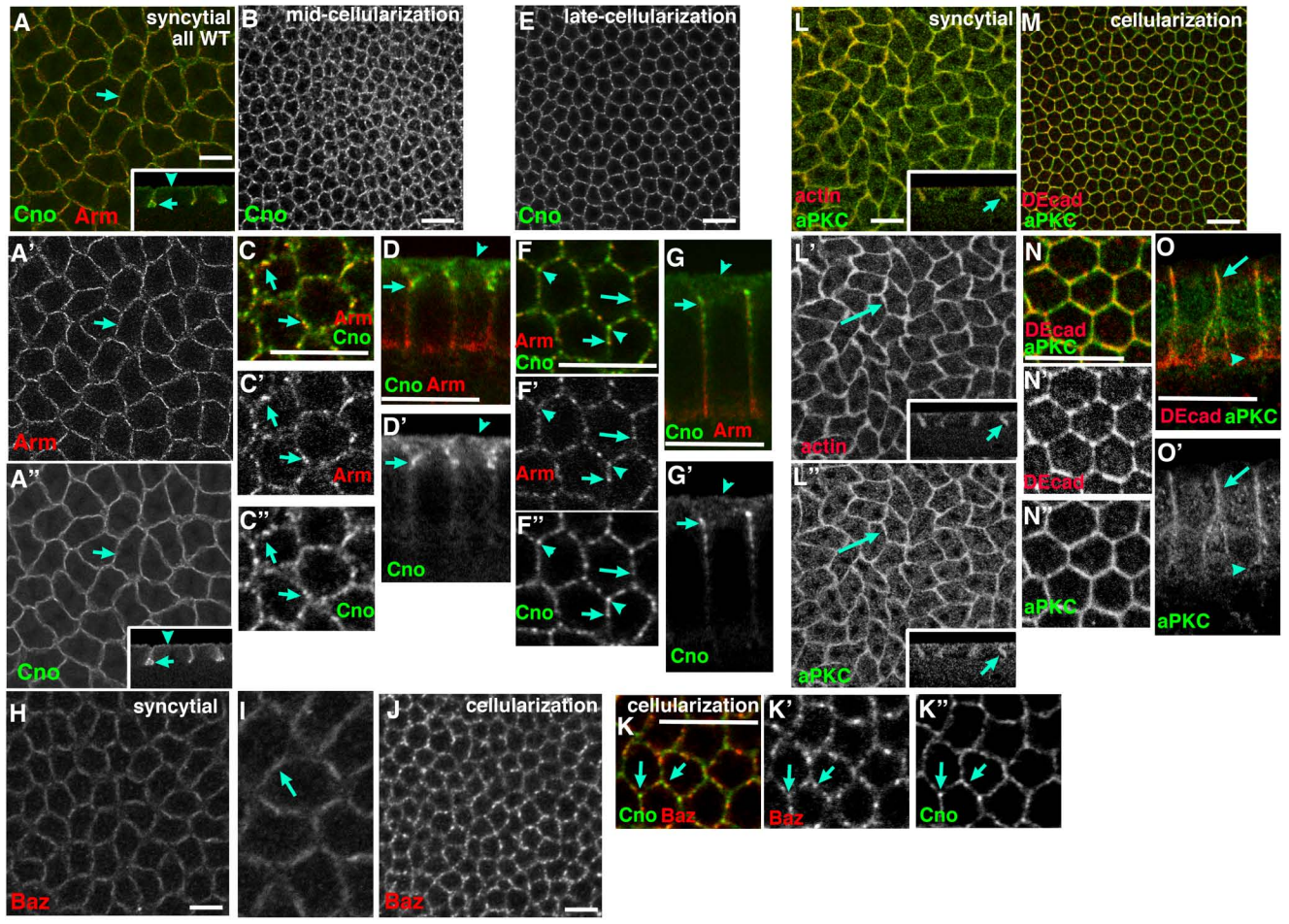
A
syncytial
all WT
Cno Arm
B
mid-cellularization
Cno
E
late-cellularization
Cno
L
syncytial
actin
aPKC
M
cellularization
DEcad
aPKC
A'
Arm
C
Arm
Cno
D
Cno Arm
F
Arm
Cno
G
Cno Arm
C'
Arm
D'
F'
Arm
G'
A''
Cno
C''
Cno
D'
Cno
F''
Cno
G'
Cno
L'
actin
L''
aPKC
N
DEcad
aPKC
O
DEcad aPKC
N'
DEcad
O'
N''
aPKC
aPKC
H
syncytial
Baz
I
J
cellularization
Baz
K
cellularization
Cno Baz
K'
Baz
K''
Cno

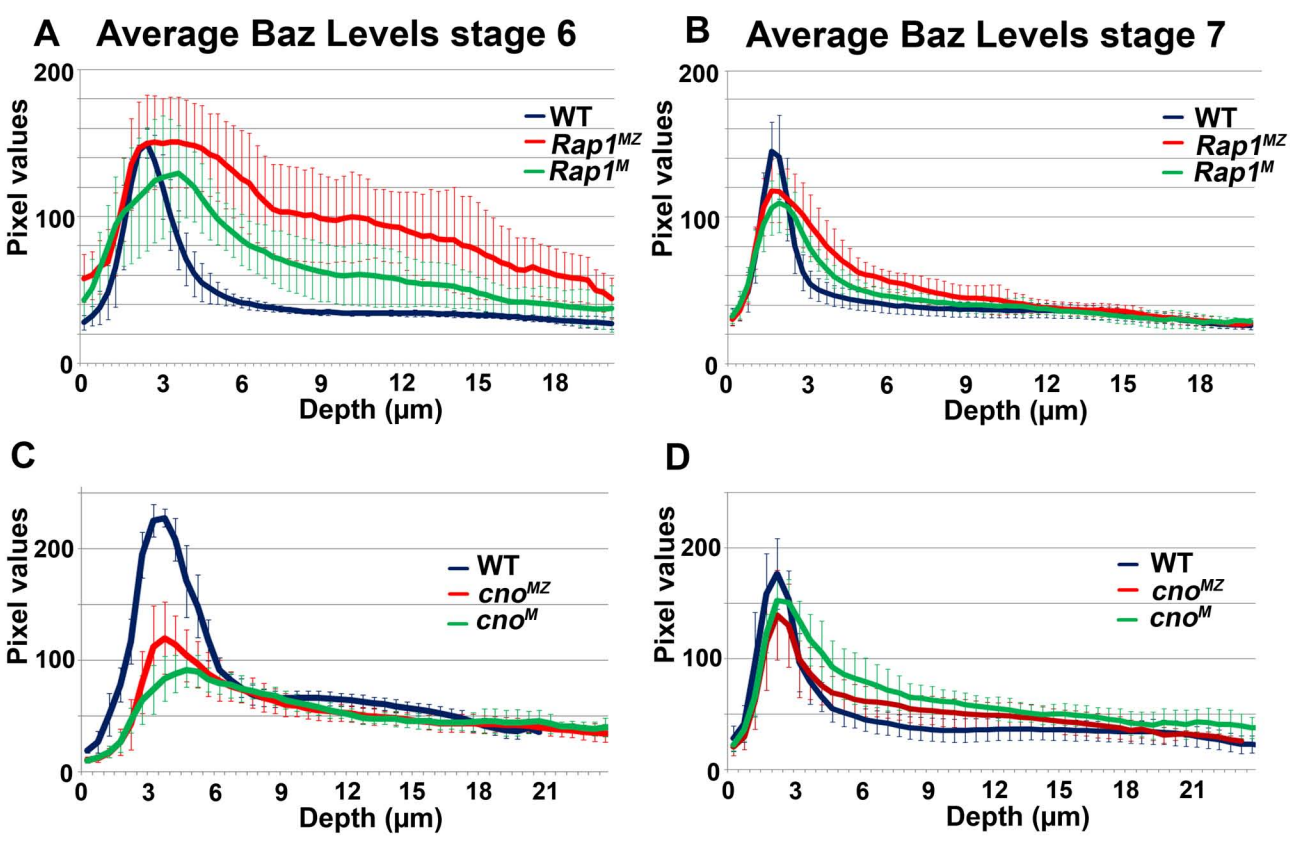
A
Average Baz Levels stage 6
Pixel values
200
100
0
0
3
6
9
12
15
18
Depth (µm)
WT
Rap1MZ
Rap1M
B
Average Baz Levels stage 7
Pixel values
200
100
0
0
3
6
9
12
15
18
Depth (µm)
WT
Rap1MZ
Rap1M
C
Pixel values
200
100
0
0
3
6
9
12
15
18
21
Depth (µm)
WT
cnoMZ
cnoM
D
Pixel values
200
100
0
0
3
6
9
12
15
18
21
Depth (µm)
WT
cnoMZ
cnoM

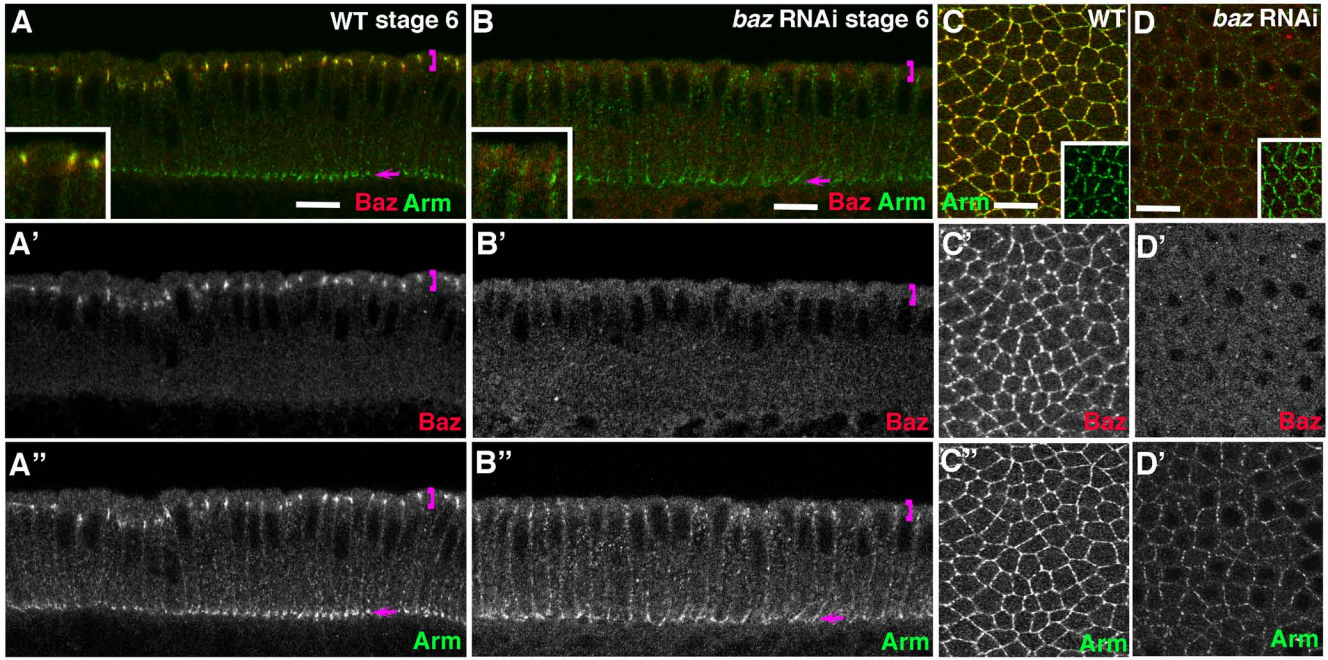
A
WT stage 6
Baz Arm
B
baz RNAi stage 6
Baz Arm
C
WT
Arm
D
baz RNAi
A'
Baz
B'
Baz
C'
Baz
D'
Baz
A''
Arm
B''
Arm
C''
Arm
D'
Arm

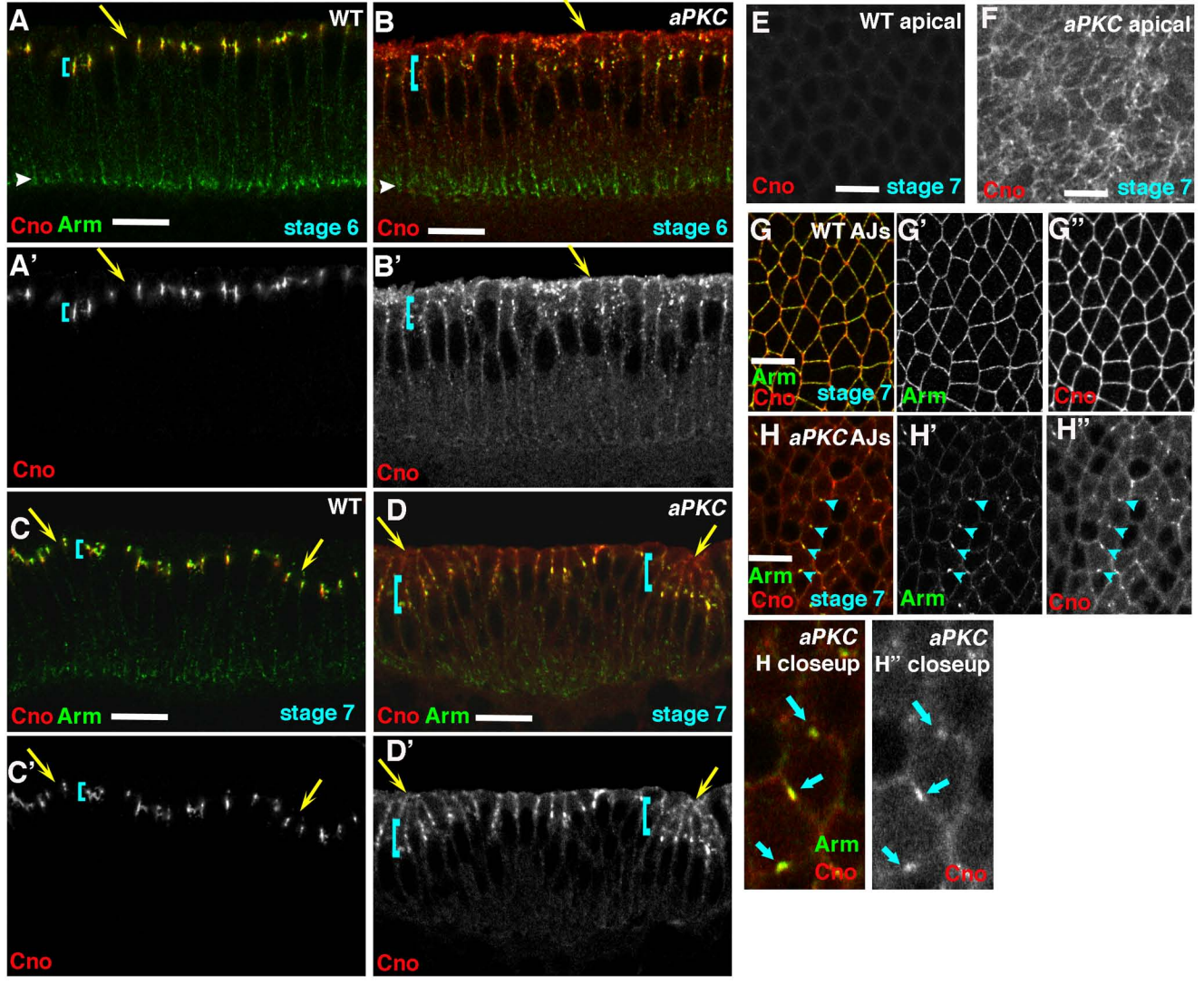
A
WT
Cno Arm
stage 6
B
aPKC
Cno
stage 6
A'
Cno
B'
Cno
C
WT
Cno Arm
stage 7
D
aPKC
Cno Arm
stage 7
C'
Cno
D'
Cno
E
WT apical
Cno
stage 7
F
aPKC apical
Cno
stage 7
G
WT AJs
Arm
Cno
stage 7
G'
Arm
G''
Cno
H
aPKC AJs
Arm
Cno
stage 7
H'
Arm
H''
Cno
aPKC
H closeup
Arm
Cno
aPKC
H'' closeup
Cno

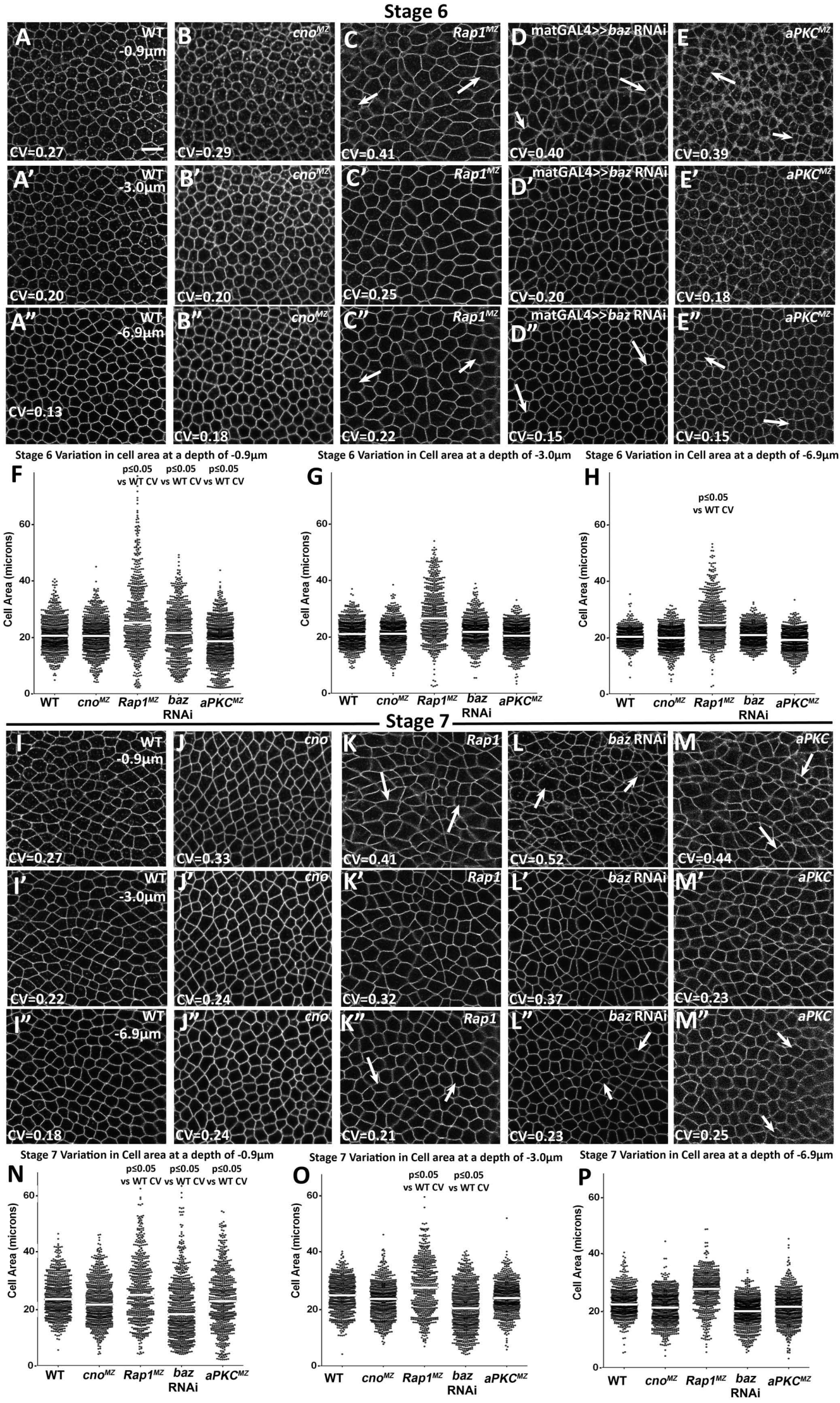
Stage 6
A
WT
-0.9µm
CV=0.27
B
cnoMZ
CV=0.29
C
Rap1MZ
CV=0.41
D
matGAL4>>baz RNAi
CV=0.40
E
aPKCMZ
CV=0.39
A'
WT
-3.0µm
CV=0.20
B'
cnoMZ
CV=0.20
C'
Rap1MZ
CV=0.25
D'
matGAL4>>baz RNAi
CV=0.20
E'
aPKCMZ
CV=0.18
A''
WT
-6.9µm
CV=0.13
B''
cnoMZ
CV=0.18
C''
Rap1MZ
CV=0.22
D''
matGAL4>>baz RNAi
CV=0.15
E''
aPKCMZ
CV=0.15
Stage 6 Variation in cell area at a depth of -0.9µm
F
p≤0.05 vs WT CV
p≤0.05 vs WT CV
p≤0.05 vs WT CV
Cell Area (microns)
WT
cnoMZ
Rap1MZ
baz RNAi
aPKCMZ
Stage 6 Variation in Cell area at a depth of -3.0µm
G
Cell Area (microns)
WT
cnoMZ
Rap1MZ
baz RNAi
aPKCMZ
Stage 6 Variation in Cell area at a depth of -6.9µm
H
p≤0.05 vs WT CV
Cell Area (microns)
WT
cnoMZ
Rap1MZ
baz RNAi
aPKCMZ
Stage 7
I
WT
-0.9µm
CV=0.27
J
cno
CV=0.33
K
Rap1
CV=0.41
L
baz RNAi
CV=0.52
M
aPKC
CV=0.44
I'
WT
-3.0µm
CV=0.22
J'
cno
CV=0.24
K'
Rap1
CV=0.32
L'
baz RNAi
CV=0.37
M'
aPKC
CV=0.23
I''
WT
-6.9µm
CV=0.18
J''
cno
CV=0.24
K''
Rap1
CV=0.21
L''
baz RNAi
CV=0.23
M''
aPKC
CV=0.25
Stage 7 Variation in Cell area at a depth of -0.9µm
N
p≤0.05 vs WT CV
p≤0.05 vs WT CV
p≤0.05 vs WT CV
Cell Area (microns)
WT
cnoMZ
Rap1MZ
baz RNAi
aPKCMZ
Stage 7 Variation in Cell area at a depth of -3.0µm
O
p≤0.05 vs WT CV
p≤0.05 vs WT CV
Cell Area (microns)
WT
cnoMZ
Rap1MZ
baz RNAi
aPKCMZ
Stage 7 Variation in Cell area at a depth of -6.9µm
P
Cell Area (microns)
WT
cnoMZ
Rap1MZ
baz RNAi
aPKCMZ

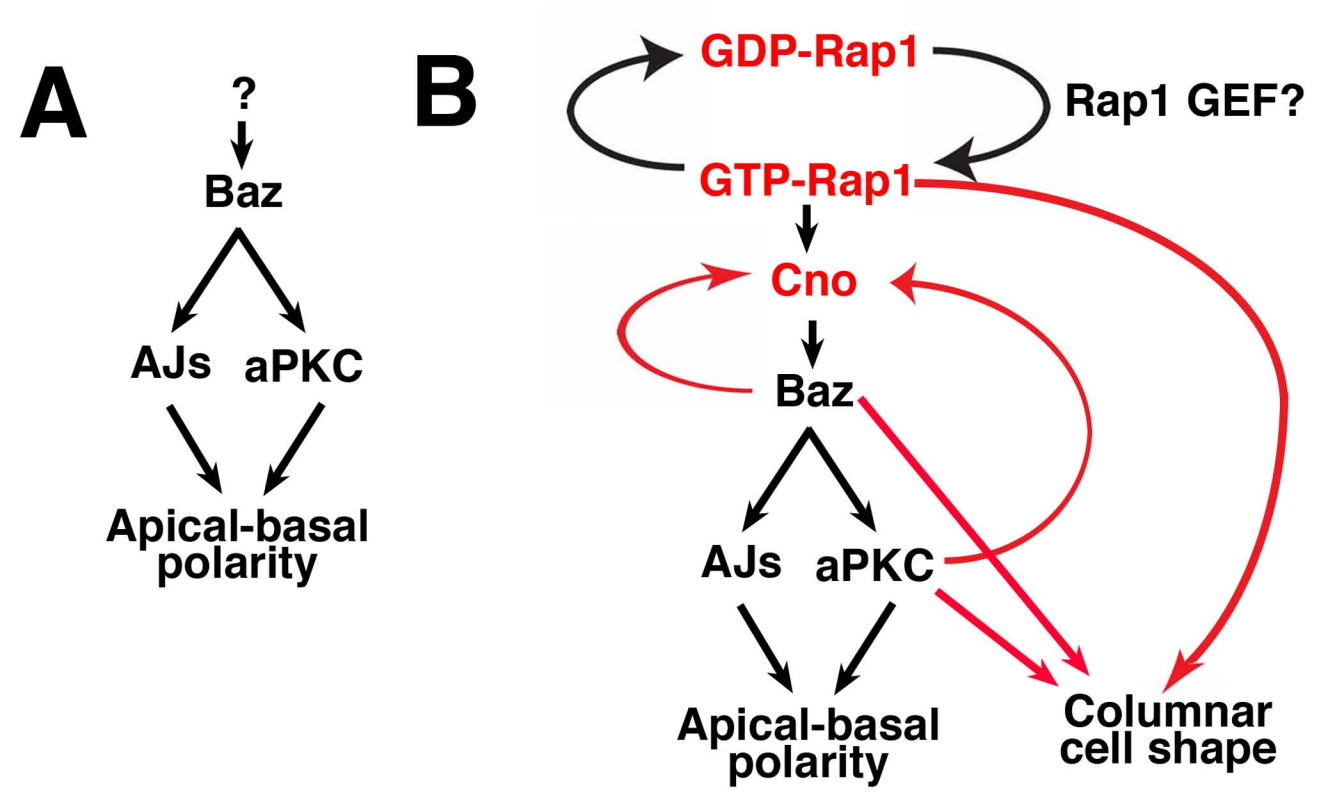
A
?
Baz
AJs
aPKC
Apical-basal polarity
B
GDP-Rap1
Rap1 GEF?
GTP-Rap1
Cno
Baz
AJs
aPKC
Apical-basal polarity
Columnar cell shape